IET Microwaves, Antennas & Propagation

Research Article

IET Journals
The Institution of Engineering and Technology

Design and fabrication of two-port three-beam switched beam antenna array for 60 GHz communication

ISSN 1751-8725
Received on 2nd November 2018
Revised 27th February 2019
Accepted on 12th March 2019
E-First on 10th April 2019
doi: 10.1049/iet-map.2018.6010
www.ietdl.org

Yuqiao Liu[1] ✉, Oday Bshara[1], Ibrahim Tekin[2], Christopher Israel[3], Ahmad Hoorfar[3], Baris Taskin[1], Kapil R. Dandekar[1]

[1]*Electrical and Computer Engineering Department, Drexel University, 3141 Chestnut Street, Philadelphia, PA, 19104, USA*
[2]*Electronics Engineering, Sabanci University, 34956 Orhanli, Istanbul, Turkey*
[3]*ECE Department, Villanova University, Villanova, PA, 19085, USA*
✉ *E-mail: yl636@drexel.edu*

Abstract: This article presents a novel, low-cost, beam-switchable 2×10 antenna array system operating at 60 GHz. This antenna system is constructed of two rows of Chebyshev-tapered microstrip antenna arrays. Each row is a 10 element series-fed array which are fed by a 90° coupler. The designed antenna array has only two input ports, but it is capable of generating three switchable beams. This antenna system can spatially scan 90° with at least −5 dB normalised gain using only one SPDT switch and a single transceiver. The maximum gain realised by the system was measured as 16.4 dBi and the bandwidth (BW) was >1 GHz. The features of the proposed antenna system make it applicable to do mmWave research such as beamforming algorithms and channel sounding, and to use in handsets for 5G communication.

1 Introduction and related work

The massive growth of mobile data and the increasing demand for higher data rates that exceed the channel capacity of 4G and long-term evolution (LTE) [1] have motivated next generation (5G) cellular systems. New technologies such as cell densification, massive MIMO, and mmWave are forming the backbone of 5G. Regarding mmWave spectrum, high gain and beam steerable antenna arrays are necessary to overcome significant free space path loss, atmospheric attenuation, and blockage by foliage at high frequencies [2, 3].

Smart antenna systems, including switched-beam systems and adaptive array systems, both can be electronically steered to point in different directions without physically moving the antennas. Smart antenna systems are the key technology to tackle the challenges in mmWave bands. On one hand, adaptive array systems are able to fully adapt to mobile channel environments in real time by generating an optimal radiation pattern that can maximise their main lobe and minimise interference. On the other hand, switched beam systems are fed by an analogue beamformer which requires a smaller number of transceivers, resulting in reduced system complexity and cost.

Given the pros and cons of analogue and digital beamforming, there should be a trade-off in order to balance between performance with real-time signal processing, power consumption, cost and system complexity by utilising hybrid beamforming [4], in which a switched-beam antenna array acts as a subsystem [5, 6]. Passive multibeam arrays (PMBAs) based on beam forming circuits are much less complex compared with phase-shifter based switched-beam antennas [7] and the array deploying the local oscillator (LO) phase-shifting approach. However, when the user position is between two adjacent beams, corresponding selection rules and possible SINR reduction need to be taken into account [3].

Usually, an $N \times N$ beamforming network with N inputs and N outputs can only generate N beams. The work in [8–10] used a 4×4 butler matrix to generate four fixed beams. Other previous works [11, 12] designed 3×3 beamformers that have enabled three direction beamforming with much simpler hardware. However, they needed more than two hybrid couplers and several phase shifters to implement the three-port beamforming network. When the number of input ports comes down to only two, beamforming networks become a 90° hybrid coupler which produces two outputs with a phase increment of $\pm 90^{\circ}$.

Here, we designed a low complexity 60 GHz antenna system for 5G mobile user equipment (UE). Previous research generated only M beams out of an $M \times N$ array, which means that, using this approach, one would need a $3 \times N$ array to generate three beams and a four by N array to generate four beams. The novelty of our solution allows for the generation of three beams from a simple $2 \times N$ array. The solution can potentially be extended to generating $M \times 2$ beams out of an $M \times N$ array. Our design has a feeding circuit with an uncommon use of an SPDT switch. Usually, a SPDT switch is connected to one of the outputs at a time. However, our switch has an additional state when both control bins are enabled at the same time. This state generates the additional third beam. Fig. 1 depicts the generated beams. When we feed the system at port 1, we get Beam 1. When we feed the system at port 2, we generate Beam 3. When we divide the input signal power and pass it into ports 1 and 2, we get Beam 2. The feeding network outputs are 0°, or $\pm 90^{\circ}$ phase difference. Then, the signals with the proper magnitude and phase difference propagate into a two-row series-fed microstrip antenna array with 10 elements each working at 60 GHz in order to achieve the high gain that mmWave communication requires.

The remaining parts of this paper are organised as below: Section 2 is a system overview, Section 3 describes our antenna design and the fabrication process, Section 4 depicts the measurements and the antenna performance, Section 5 concludes our work.

2 System overview

It is well known that the circuit of a quadrature hybrid coupler can be decomposed into the superposition of an even-mode and an odd-mode excitation [13]. When excited from a single port, the coupler is working at both modes, making the other input port isolated. When excited from both ports by the same signal, the coupler is working at even-mode only. The symmetric structure and even mode excitation produce a virtual open circuit at the centre of Z_0 stubs, which separates the two signal paths. Therefore, at the output ends, both output signals having the same magnitude and phase,

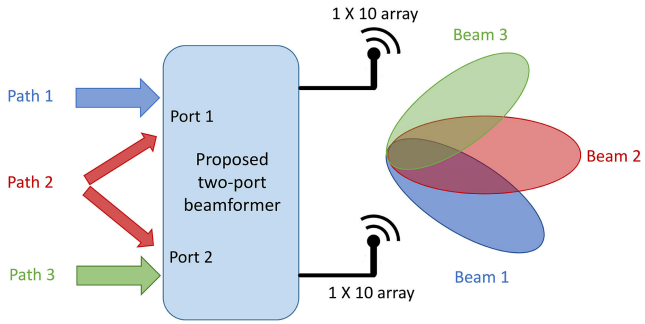

Fig. 1 *Overview diagram of the proposed antenna array system. Each antenna symbol stands for a 1 × 10 antenna array. Feeding through port 1 results in Beam 1. Feeding through port 2 results in Beam 3. Signal is fed to both ports to generate Beam 2*

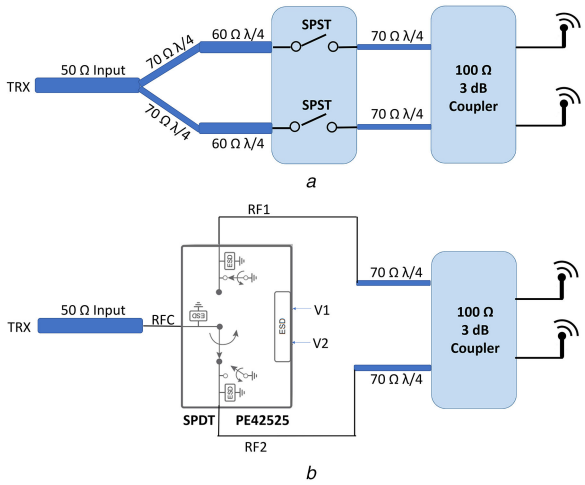

Fig. 2 *Power divider and SPDT setup structure to generate 3 beams out of 2 antenna arrays. Every antenna element symbol represents a 1 × 10 antenna array*
(a) PD+SPST
(b) SPDT chip

produce an RF signal with 0° phase difference fed to the antenna arrays.

Switching circuits are designed to switch among different excitation modes to generate the three beams. There are two possible switching circuit solutions: as shown in Fig. 2: First option is to use a power divider (PD) and two SPST switches. This design leaves one of the output ports of the PD as an open circuit. In order to deal with this open-circuit issue, we extended the outputs of the PD by 60 Ω quarter-wavelength transmission lines before connecting it to the SPST in order to ensure that, for the PD, the insertion loss is (−1 dB) and the reflection coefficient is (−15 dB). Second, the circuit in Fig. 3 uses commercially available SPDT switch chips such as PE42525 from Peregrine Semiconductor [14]. Fig. 3 shows the principle of operation: When only one of the control signals V1 or V2 is high, the antenna system is able to generate beam 1 or beam 3; When the control signals V1 and V2 are both high, the RF paths 1 and 2 are all turned on according to the truth table from the datasheet of PE42525 chip. Thus, the signal is fed to both input ports, generating beam 2.

3 Design and fabrication

The antenna system was designed based on microstrip transmission lines (MTLs). In order to reduce the fabrication cost, no vias were needed except for the connector-mounting area. Considering both cost and loss, two-layer 0.2 mm (8 mil) thickness RO4003 laminate was selected as a substrate which was thin enough to avoid any unexpected higher order modes and surface waves. The design initially ran through an extensive simulation process for its critical components such as the 90° coupler, the single patch antenna, and

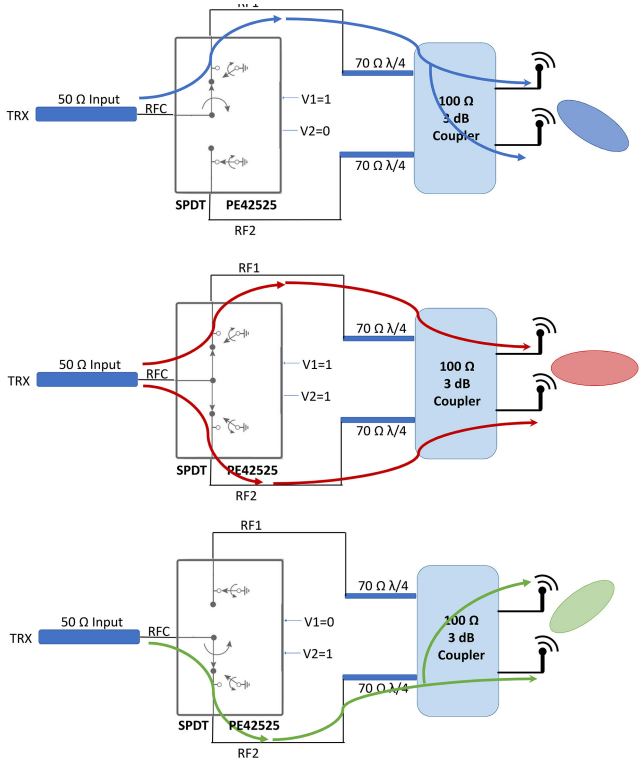

Fig. 3 *SPDT setup structure to generate 3 beams out of 2 antenna arrays. Every antenna element symbol represents an 1 × 10 antenna array. Colour scheme is the same as the one in Fig. 1. Each colour represents one switching option that generates a beam*

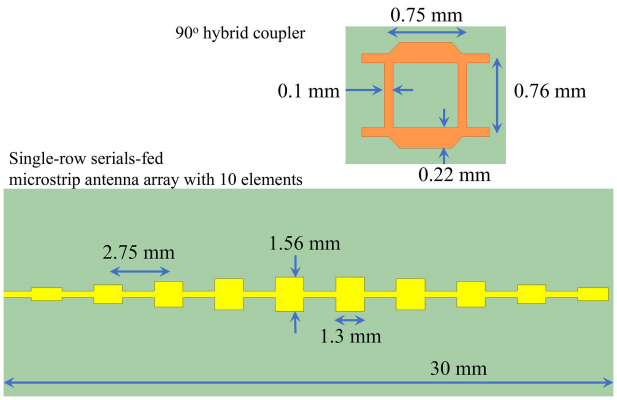

Fig. 4 *Dimensions of 90° hybrid coupler and single row antenna array*

the single row 1 × 10 antenna array with the help of ANSYS high-frequency structure simulator (HFSS) version 19.1.

The dimension and structure of the key components are shown in Fig. 4. The coupler was designed using $Z_0 = 100\ \Omega$ characteristic impedance system. This Z_0 choice was made after comparing the quarter wavelength of 100 and 50 Ω MTLs. 50 Ω quarter wavelength MTL would have been large and would have caused coupling between transmission lines.

Series-fed microstrip antennas are commonly used due to their simple feed line compared with complex corporate-fed networks. We first designed a single half-wavelength patch operating at 60 GHz. Then, in order to implement 50 Ω input impedance, we took advantage of the high propagation loss at mmWave band to feed the patches from the edges by half-wavelength MTLs. After connecting the first element to the other nine half-wavelength patches and nine half-wavelength MTLs, the whole structure stays resonant at 60 GHz, but the resonant impedance reduces from 300 Ω [13], with only one element, to 50 Ω with 10 elements as the return loss plot shows in Fig. 5. Then, the widths of each patch are tapered using Chebyshev polynomials for equal side lobe level in magnitude. The tapering ratio is 1 : 0.91 : 0.74 : 0.54 : 0.38 from

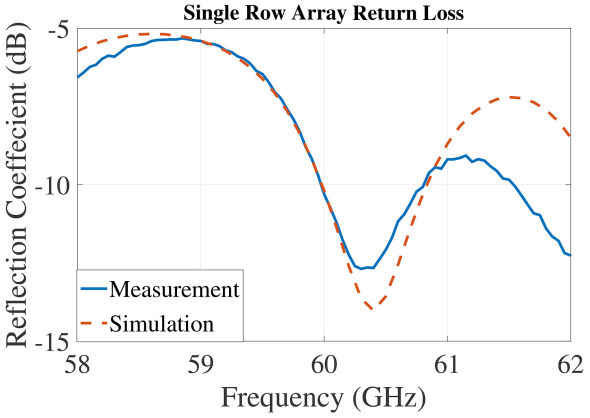

Fig. 5 *Comparison of simulated and measured return loss of a 1 × 10 array*

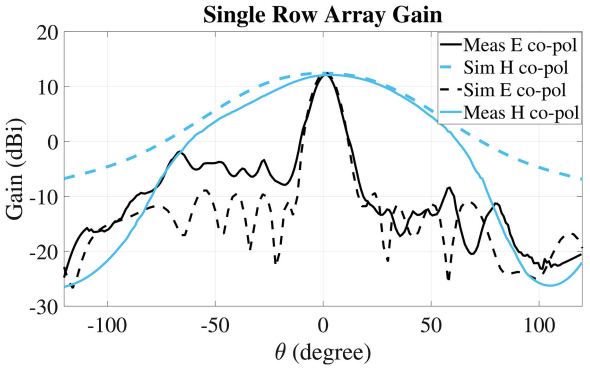

Fig. 6 *R1.2: Comparison of simulated and measured gain of a 1 × 10 array at 60.4 GHz*

the centre patch to edge to ensure that the side-lobe level is 20 dB lower than the main beam in the *E* plane. We used 1.3 mm for the length of patch elements, 0.1 mm shorter than half-wavelength due to the fringing fields near the edge of each patch, we also used approximately half-wavelength (1.45 mm) long, 0.3-mm-wide MTLs to connect patches together. The distance between adjacent patch elements is 2.75 mm, which is about 0.55 wavelength in the air. The performance of the single-row array was validated before taking the measurements of the whole system. The reflection coefficient plots in Fig. 5 R1.3: shows −10 dB bandwidth (BW) of 1 GHz and Fig. 6 plots the antenna gain in both *E* and *H* planes, showing a maximum gain of 12.14 dBi at 60.4 GHz.

Although a two-layer board can be used for fabrication, we decided to use a four-layer stacked structure in order to enhance mechanical strength. The stack structure of the PCB is shown in Fig. 7: the first layer is half oz copper for the transmission lines and patches, the second copper layer is a whole ground plane made with half oz copper, while the third and fourth layers have copper only for connector mounting. 8 mil RO4003C laminate was used between the first and second layers as well as between the third and fourth layers. We used 4-mil-thick RO4350B between the second and the third layers. Electroless Nickel with Immersion Gold coating (ENIG) was chosen as a surface finishing process for the purpose of avoiding corrosion. Fig. 8 shows the fabricated two row antenna connected to the output of a coupler.

4 Performance of antenna system

In order to evaluate the performance of our design, we initially characterised port isolation and return loss by collecting *S* parameter measurements of the 2 × 10 array using a Keysight PNA-X N5247 10 MHz–67 GHz network analyser in the Drexel wireless systems laboratory (DWSL). Fig. 9 shows <−15 dB return loss from 59 to 62 GHz as well as <−15 dB isolation between input ports from 59.5 to 61.5 GHz.

Radiation performances of the proposed antenna system were measured in the anechoic chamber (compact range) of the antenna

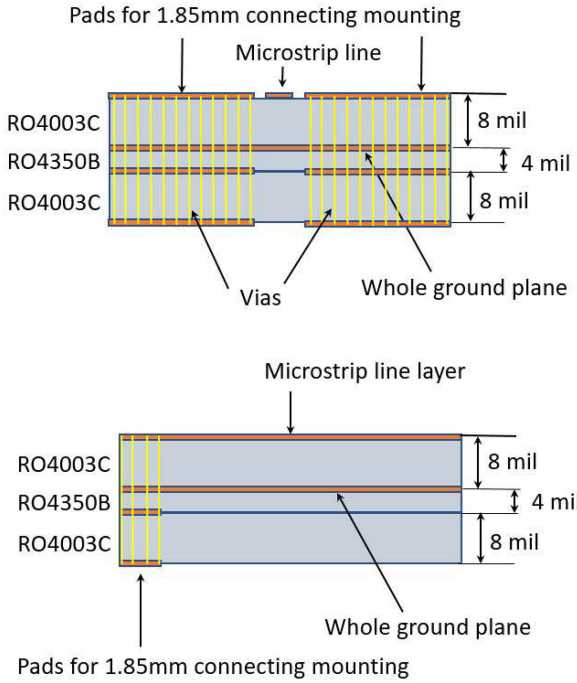

Fig. 7 *Front view (top) and side view (bottom) of 4-layer PCB stack structure*

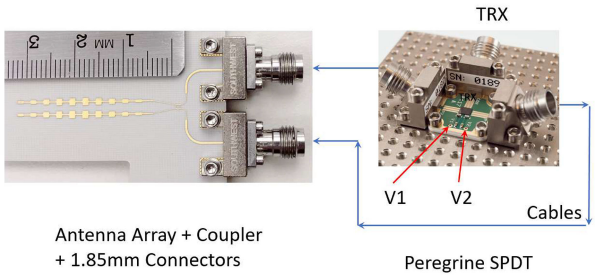

Fig. 8 *Top view of the fabricated two row antenna connected to the output of a coupler with an SPDT chip*

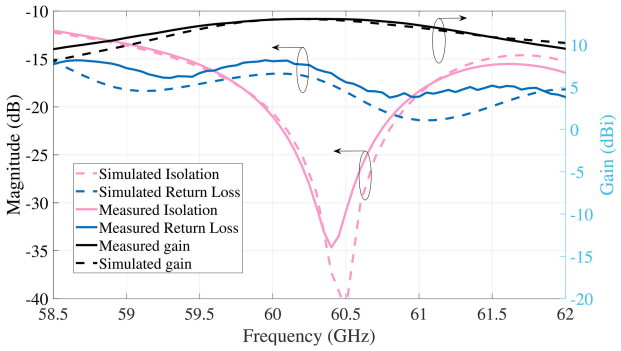

Fig. 9 *R1.2: (Left axis) S parameter comparison between simulation and measurements of final design showing the isolation between two input ports and the return loss; (Right axis) Realised gain over the frequency range. It has a gain peak at 60.2 GHz*

research laboratory (ARL) at Villanova University. The measurement device under test (DUT) comprises the fabricated 2 × 10 antenna array connected to the 90° coupler, two Southwest 1892-04A-61.85 mm End Launch Low Profile connectors, coaxial cables, and a Pulsar PS2-57-450/15S two-way PD. Insertion loss of the components other than the antenna system was compensated for through measurement system calibration.

From the anechoic chamber measurements shown in Fig. 9 (right), we can see the maximum system gain is over 12 dBi covering the frequency range from 59.5 to 61.3 GHz, while maximum gain was 12.93 dBi at 60.2 GHz. R1.1: The simulated

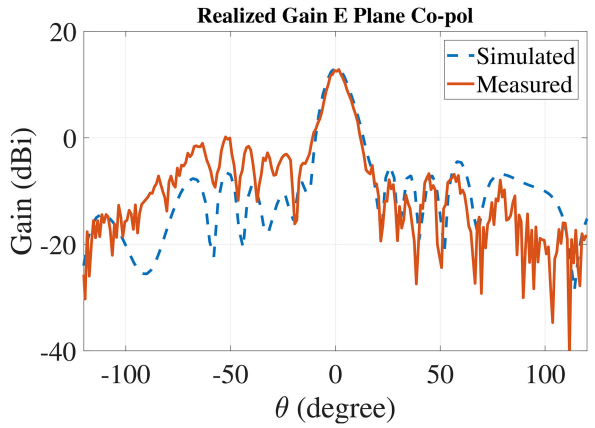

Fig. 10 *Comparison of simulated and measured realised gain in E plane of proposed antenna system fed from both ports*

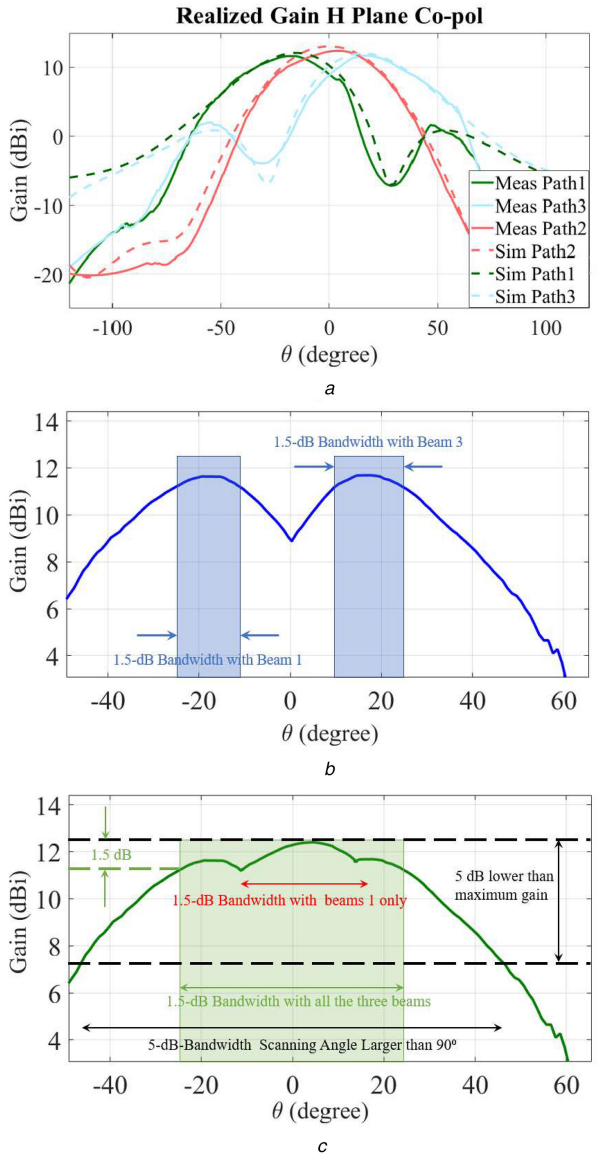

Fig. 11 *R1.1:*
(a) Comparison of simulated and measured radiation patterns of three beams in the *H* plane of the proposed antenna system. ***(b)*** Combined radiation pattern with conventional 2 by 2 beam former (with beam 1 and beam 3 only). ***(c)*** Combined radiation pattern with additional beam at the centre using proposed beam former. It is obvious that a phase shift of ±90° causes a beam shift by ±20°. Also, beam scanning angle is larger than 90° when the threshold set to be 5 dB lower than maximum gain. With additional beam at the centre, the 1.5 dB bandwidth increases by 70%

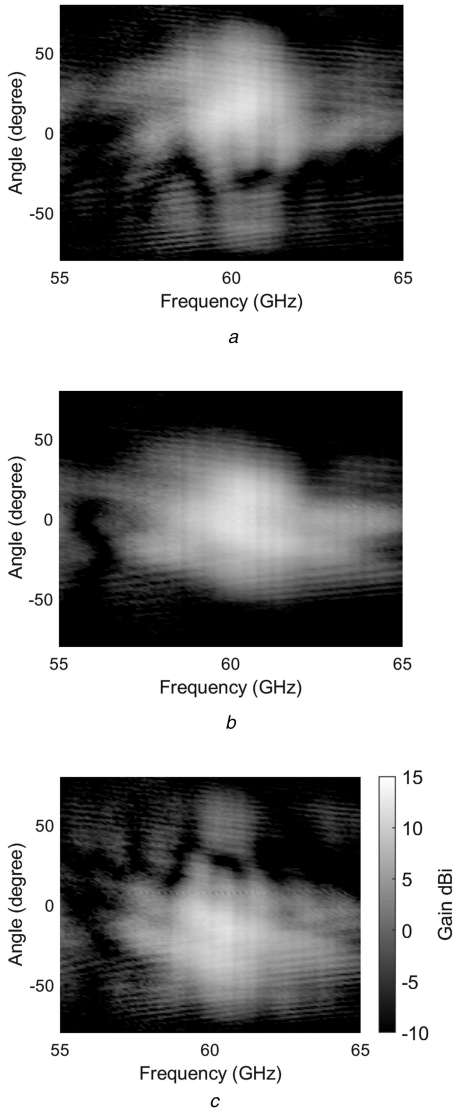

Fig. 12 *R1.1 and R1.2: Experimental measurement of the angular scan of the three generated beams over frequency. Beam numbers follow the naming convention in Fig. 1*
(a) Beam 3
(b) Beam 2
(c) Beam 1

and measured radiation patterns of *E* and *H* planes are presented in Figs. 10 and 11, respectively. It can be seen in the *E* plane, side lobes on the right side are −20 dB less than the main lobe thanks to the tapering technique. The side lobes at the left side are a little bit higher due to the spurious radiation of feed junctions. R1.1: Although in the *E* plane, the beams are not steered, variable patterns in the *H* plane are obtained by exciting from different single ports or from both ports. The maximum gains at 60 GHz were observed at θ equals 20°, 0°, and −20°. The angular coverage and frequency response of the antenna system was measured and presented in Fig. 12. R1.1: In ideal cases, assuming all the beams can get switched in order to achieve optimised gain, we are able to plot combined gain as shown in Figs. 11*b* and *c*. It is clear in Fig. 11*b* with only conventional beam 1 and beam 3, there is a notch at 0° spatial angle. The 1.5 dB BW with all the three possible beams generated by the proposed antenna system is about 50°, which is 70% larger than the antenna system with conventional beams.

The low-cost ENIG-coating helps to protect the copper from being corroded. However, due to the existence of nickel and significant skin-effect in mmWave bands, the conductive loss becomes much higher than it is in pure copper. HFSS simulations shows the gain decrease when adding a nickel layer on top of copper traces. As seen from Table 1, while simulated and

Table 1 Comparison of simulated and measurement results with and without ENIG

	Simulation with pure copper, dBi	Simulation with ENIG, dBi	Fabricated with ENIG, dBi
1 × 10 antenna	14.5	12.3	12.14
state 1 or 3	16.4	13.12	12.93
state 2	15.6	12.26	12.20

measurement results match, there is almost 3 dB loss when comparing the cases that copper is coated or not. We believe, if using hard gold coating, that the maximum gain of the proposed antenna array can be at least 16 dBi.

5 Conclusion

This paper provides simulation and anechoic-chamber measurement results for our low-cost switched-beam antenna array at 60 GHz. The antenna has been designed to serve in a 5G mobile handset in the 60 GHz band. The designed antenna is capable of switching among three beams. Two of the beams are generated by feeding through one port of the 2×10 antenna array, while the third beam is generated through feeding both antenna arrays to allow a third beam. Antenna switching feature that this antenna configuration provides can be used to perform wide beam scanning during initial beam search or during handover process in a 5G-enabled cellular network.

6 Acknowledgment

This work was supported by U.S. Office of Naval Research (ONR) under award number N00014-16-1-2037.

7 References

[1] Rappaport, T.S., Sun, S., Mayzus, R., *et al.*: 'Millimeter wave mobile communications for 5G cellular: it will work!', *IEEE. Access.*, 2013, **1**, pp. 335–349

[2] Shafi, M., Molisch, A.F., Smith, P.J., *et al.*: '5G: a tutorial overview of standards, trials, challenges, deployment, and practice', *IEEE J. Sel. Areas Commun.*, 2017, **35**, (6), pp. 1201–1221

[3] Hong, W., Jiang, Z.H., Yu, C., *et al.*: 'Multibeam antenna technologies for 5G wireless communications', *IEEE Trans. Antennas Propag.*, 2017, **65**, (12), pp. 6231–6249

[4] Han, S., Chih-Lin, I., Xu, Z., *et al.*: 'Large-scale antenna systems with hybrid analog and digital beamforming for millimeter wave 5G', *IEEE Commun. Mag.*, 2015, **53**, (1), pp. 186–194

[5] Garcia-Rodriguez, A., Venkateswaran, V., Rulikowski, P., *et al.*: 'Hybrid analog–digital precoding revisited under realistic RF modeling', *IEEE Wirel. Commun. Lett.*, 2016, **5**, (5), pp. 528–531

[6] Venkateswaran, V., Pivit, F., Guan, L.: 'Hybrid RF and digital beamformer for cellular networks: algorithms, microwave architectures, and measurements', *IEEE Trans. Microw. Theory Tech.*, 2016, **64**, (7), pp. 2226–2243

[7] Seyyed Esfahlan, M., Öztürk, E., Kaynak, M., *et al.*: '77-GHz Four-element phased-array radar receiver front end', *IEEE Trans. Compon. Packag. Manuf. Technol.*, 2016, **6**, (8), pp. 1162–1173

[8] Tseng, C.H., Chen, C.J., Chu, T.H.: 'A low-cost 60-GHz switched-beam patch antenna array with butler matrix network', *IEEE Antennas Wirel. Propag. Lett.*, 2008, **7**, pp. 432–435

[9] Yang, Q.L., Ban, Y.L., Lian, J.W., *et al.*: 'SIW butler matrix with modified hybrid coupler for slot antenna array', *IEEE. Access.*, 2016, **4**, pp. 9561–9569

[10] Liu, Y., Bshara, O., Tekin, I., *et al.*: 'A 4 by 10 series 60 GHz microstrip array antenna fed by butler matrix for 5G applications'. In 2018 IEEE 19th Wireless and Microwave Technology Conf. (WAMICON), Sand Key, FL, USA, April 2018, pp. 1–4.

[11] Ding, K., Fang, X., Wang, Y., *et al.*: 'Printed dual-layer three-way directional coupler utilized as 3×3 beamforming network for orthogonal three-beam antenna array', *IEEE Antennas Wirel. Propag. Lett.*, 2014, **13**, pp. 911–914

[12] Odrobina, S., Staszek, K., Wincza, K., *et al.*: 'Broadband 3×3 butler matrix'. In 2017 Conf. on Microwave Techniques (COMITE), Brno, Czech Republic, April 2017, pp. 1–5

[13] Pozar, D.M.: '*Microwave engineering*' (Wiley Global Education, San Diego, CA, USA, 2011, 4th edn.)

[14] 'Peregrine semiconductor PE42525 specification', 2016, https://wwwpsemicom/pdf/datasheets/pe42525dspdf